

## THE HARD X-RAY BEHAVIOR OF AQL X-1 DURING TYPE-I BURSTS

YU-PENG CHEN<sup>1</sup>, SHU ZHANG<sup>1</sup>, SHUANG-NAN ZHANG<sup>1</sup>,  
LONG JI<sup>1</sup>, DIEGO F. TORRES<sup>2,3</sup>, PETER KRETSCHMAR<sup>4</sup>, JIAN LI<sup>1</sup>, JIAN-MIN WANG<sup>1,5</sup>

*Draft version June 20, 2021*

### ABSTRACT

We report the discovery of an anti-correlation between the soft and the hard X-ray lightcurves of the X-ray binary Aql X-1 when bursting. This behavior may indicate that the corona is cooled by the soft X-ray shower fed by the type-I X-ray bursts, and that this process happens within a few seconds. Stacking the Aql X-1 lightcurves of type-I bursts, we find a shortage in the 40–50 keV band, delayed by  $4.5 \pm 1.4$  s with respect to the soft X-rays. The photospheric radius expansion (PRE) bursts are different in that neither a shortage nor an excess shows up in the hard X-ray lightcurve.

*Subject headings:* stars: coronae — stars: neutron — X-rays: individual(Aql X-1) — X-rays: binaries — X-rays: bursts

### 1. INTRODUCTION

A low-Mass X-ray Binary (LMXB) is a system with either a neutron star (NS) or a black hole (BH) accreting material from a companion star (in general having a mass  $M \leq M_{\odot}$ ), usually via a Roche-Lobe overflow settling into an accretion disk. Many LMXBs show periods of high activities, referred to as outbursts, which are probably triggered by changes in the mass accretion rate. Basically, there are two components (an optically thick blackbody like component in the soft X-ray band and a power law with cutoff component in the hard X-ray band) in the outburst spectrum of a LMXB. It is thought that the power law component is caused by inverse Comptonization of the hot plasma (i.e. the corona, see the case of 4U 1608–522 Zhang et al. 1996); the seed photons being the optically thick blackbody like component. However, no consensus has been reached on the corona formation model, and both disk evaporation (Meyer et al. 1994; Esin et al. 1997; Liu et al. 2007; Frank et al. 2002) and magnetic reconnection models (Zhang et al. 2000; Mayer & Pringle 2007; Zhang 2007) are entertained. The timescale of the corona formation/heating is key to distinguish between these models. The typical timescale for disk evaporation and magnetic reconnection models are days (Meyer et al. 1994; Esin et al. 1997; Liu et al. 2007; Frank et al. 2002) and milliseconds (Zhang et al. 2000; Mayer & Pringle 2007; Zhang 2007), respectively.

Type-I X-ray bursts are caused by unstable burning of the accreted hydrogen/helium on the surface of a NS enclosed in an XRB, and manifest themselves as a sudden increase (typically by a factor of 10 or greater) in the X-ray luminosity followed by an exponential de-

cay (for reviews, see Lewin et al. 1993; Cumming 2004; Strohmayer & Bildsten 2006; Galloway et al. 2008). The most luminous bursts are the photospheric radius expansion (PRE) events, for which the peak flux is comparable to the Eddington luminosity at the surface of the NS.

The spectral behavior of the outbursts (i.e., persistent/accretion emission from the accretion disk and corona) might be affected by the bursts themselves. In fact, a hard X-ray flux decrease was hinted at during a burst of Aquila X-1 (Aql X-1, also named 4U 1908+005) observed with RXTE/HEXTE, but with a significance of only  $\sim 2 \sigma$  (Maccarone & Coppi 2003). Effects at energies lower than 30 keV were reported by Worpel et al. (2013); Zand et al. (2013).

Aql X-1 is a transient NS XRB, classified as an atoll source (Reig et al. 2000). It is one of the three NS XRBs which show hysteresis in state transition (Gladstone et al. 2007); the other two being 4U 1608-522 (Maitra & Bailly 2004) and IGR J17473-2721 (Zhang et al. 2009; Chen et al. 2010, 2011). Tens of type-I bursts were detected during the outbursts of Aql X-1. Among them, roughly one third are PRE bursts (Galloway et al. 2008). In this paper, we report on a detailed analysis of all RXTE/PCA observations on Aql X-1, with the aim of gathering information about the timescales of formation of its corona.

### 2. OBSERVATIONS AND RESULTS

#### 2.1. Bursts selection

Aql X-1 was frequently monitored by RXTE during its service till 2012. The analysis of the PCA data is performed using HEASoft v.6.6. The data are filtered using the standard RXTE/PCA criteria. Only the data from the PCU2 (the third Proportional Counters Unit, in the 0-4 numbering scheme) are used for the analysis, because this PCU was 100% on during all the observations. The dead time correction is made to all the spectra and lightcurves following the standard procedure described at the HEASARC website.

From all available RXTE/PCA pointing observations on Aql X-1, we carried out a systematic search for bursts in the lightcurve of Aql X-1. Only the bursts observed by PCA in E\_125u\_64M\_1s mode (events are time-stamped

Electronic address: chenyp@ihep.ac.cn, szhang@ihep.ac.cn

<sup>1</sup> Key Laboratory for Particle Astrophysics, Institute of High Energy Physics, Chinese Academy of Sciences, 19B Yuquan Road, Beijing 100049, China

<sup>2</sup> Institució Catalana de Recerca i Estudis Avançats (ICREA), 08010 Barcelona, Spain

<sup>3</sup> Institute of Space Sciences (IEEC-CSIC), Campus UAB, Torre C5, 2a planta, 08193 Barcelona, Spain

<sup>4</sup> European Space Astronomy Centre (ESA/ESAC), Science Operations Department, Villanueva de la Cañada (Madrid), Spain

<sup>5</sup> Theoretical Physics Center for Science Facilities (TPCSF), CAS

with 125-microsec resolution, in 64 PHA channel bands with the ‘M’ channel distribution/binning scheme starting at channel 0, and are read out every 1 second) are chosen for analysis, which have enough energy bands and good time resolution. We picked up 39 bursts to constitute a sample, among which 13 are PRE events (Table 1).

## 2.2. Data analysis

During the bursts, the persistent/accretion and the burst emission are mixed. In order to investigate persistent/accretion emission changes during the type-I X-ray burst, we analyze the spectra and lightcurves by subtracting the pre-burst emission (including instrumental background and persistent/accretion flux of the neutron star).

The burst spectrum is well modeled by a blackbody with a characteristic temperature of a few keV. The burst emission can reach  $L_{\text{Edd}}$ , and dominates the total emission at energies well below  $\sim 40$  keV, above which the persistent/accretion emission from the corona takes over. The average of the 40–50 keV, persistent count rates recorded by RXTE/PCA for non-PRE and PRE bursts are  $0.37 \pm 0.05$  cts/s and  $0.05 \pm 0.04$  cts/s, respectively.

Because the flux in the 40–50 keV band is very faint to be detected during single bursts, especially when the instrument background is  $\sim 1$  cts/s, which is much higher than the persistent/accretion and bursts emission in the same energy band, we stack the individual lightcurves. For each burst, we use the time of its peak in the 2–10 keV as a reference to produce the lightcurve of each burst in the 2–10 keV band as well as in the 40–50 keV band. The fluxes recorded 48 seconds before and 80 seconds after the reference time are regarded as the persistent/accretion flux and are subtracted for each burst in timing analysis. The results are stable with reasonable changes of the time period where the persistent/accretion count rate is estimated. After the persistent emission is subtracted, we separate the PRE bursts from the non-PRE bursts. From the the Color-color diagram (CCD) and Hardness-Intensity diagram (HID) of Aql X-1 (Fig. 1), the non-PRE bursts and the PRE bursts are mostly located in the hard state and the soft state, respectively. Based on the CCD and HID, we subdivide the bursts into non-PRE bursts in the hard state, PRE bursts in the soft state, non-PRE bursts in the soft state and PRE bursts in the hard state. For the latter two groups, the number of bursts is too small to draw conclusion (Table 1). In this paper, only the former two groups (the non-PRE bursts in the hard state and the PRE bursts in the soft state) are stacked and averaged in each time bin, respectively.

## 2.3. Results

As shown in Fig. 2, for the non-PRE bursts in the hard state, the 40–50 keV flux of the combined 4s-binned lightcurve is mostly negative during the bursts occurrence and flat elsewhere. The 40–50 keV decrement reaches a maximum of  $-0.9 \pm 0.2$  cts/s at the 2-10 keV burst peak, which amounts to the whole 40–50 keV persistent flux. A constant fit with a 1 s-bin light curve that ranges from 0 seconds to 15 seconds results in a  $\chi^2$  of 74 under 15 dofs, suggesting a significance of  $6 \sigma$  for the shortage.

By assuming that the spectrum of the corona is well described by a cutoff power law (cutoffpow model in XSPEC) with a photon index 1.25, we simulate the PCA spectra with different cutoff energy, fixed photon index and normalization. We find that the PCA flux in 40–50 keV is 0.37 cts/s, 0.24 cts/s, 0.11 cts/s, 0.06 cts/s and 0.01 cts/s for the cutoff energy of 40 keV, 30 keV, 20 keV, 15 keV, and 10 keV, respectively. This means that the PCA flux between 40 and 50 keV can drop by about one order of magnitude if the corona temperature is cooled from 40 keV to 10 keV, resulting in a significant shortage at hard X-rays while bursting. Assuming that the hard X-rays originate from the corona, this suggests that most of the corona is cooled by the soft photons of the bursts.

We perform a cross-correlation analysis between the two light curves at 2–10 keV and 40–50 keV, with a bin size of 1 s. In this procedure, 1 s-bin lightcurves were adopted because for a smaller time interval, e.g. 0.5 s, the poor statistics prevents from estimating a time lag. The cross-correlation, see Fig. 3, shows that the shortage at 40–50 keV lags that at 2–10 keV by  $1.8 \pm 1.5$  s. In order to estimate the error, we sampled the two lightcurves by assuming that the flux in each bin has a Gaussian distribution, and estimated the time delay with a cross-correlation method. By sampling the lightcurve a thousand times, the distribution of the resulted time delay was fitted with a Gaussian to infer the error.

A similar analysis procedure is carried out on the PRE bursts in the soft state as well. In the 40–50 keV light curves, no hint of a shortage nor an excess is present around the soft X-ray peak. As shown in Fig. 2, the 40–50 keV lightcurve hovers around zero during/around the burst. A constant fit to this light curve gives a  $\chi^2$  of 9.0 under 5 dofs, consistent with no deviation.

## 3. DISCUSSION

### 3.1. Additional corona cooling by the bursts

We have found an anti-correlation of the soft and hard X-ray lightcurves of Aql X-1 when bursting, which likely indicates a cooling of the corona by the soft X-ray showers of the bursts. This reveals a cooling/heating timescale of less than a few seconds. These results are similar to those previously found for IGR J17473-2721 (Chen et al. 2012), perhaps hinting at a generic behavior of NS XRBs.

When bursts do not occur, the corona cooling is driven by the soft photons from the disk. Therefore a timescale of a few days reflects the actual timescale of the soft disk photon field, e.g. the viscous timescale of the disk. When bursts happen, their soft photons overwhelm those from the disk and provide additional cooling in a short time (typically of tens of seconds). The anti-correlation between hard and soft X-rays shows that the corona can be cooled and recovers quite fast (in seconds). Such short timescales for recovery is inconsistent with the disk evaporation model in which the formation of a corona is driven and energized by the disk accretion. Magnetic field reconnection can provide a viable alternative.

### 3.2. Persistent/accretion spectrum softens during the bursts

The PRE bursts are the most luminous events. Their fluxes can stay very close to the Eddington limit, accompanied with a drop of color temperature below 1 keV

and an increment of the apparent radius to several tens kilometer. Although PRE bursts are brighter, no anti-correlation is found at hard X-rays. The PRE bursts of Aql X-1 are mostly located in the decaying phase of the outbursts and in the banana state of the CCD diagram (Fig. 1). The persistent flux at 40–50 keV is quite low ( $0.05 \pm 0.04$  cts/s) during the PRE bursts, implying a weak corona and thus poor statistics for measuring a possible shortage.

The persistent/accretion flux in 2.5–25 keV has been found to increase by a factor of 20 during the PRE bursts of 40 sources by RXTE/PCA (Worpel et al. 2013). In their work, the possible influence of the burst upon the persistent flux was investigated via spectral fitting, where the spectrum was fitted jointly with the burst blackbody and the persistent spectral shape at 2.5–25 keV. A significant increment was derived for the persistent emission during the burst of PRE events (Worpel et al. 2013), and these authors claim that this phenomenon is also detected for the non-PRE bursts in their forthcoming paper.

If the persistent/accretion flux increased by a factor of 20 during the PRE bursts of Aql X-1, the flux of 40–50 keV ( $F_{\text{accretion}}$ ) will be up to  $0.05 \times 20$  cts/s  $\sim 1$  cts/s. Considering the number of the PRE bursts  $N_{\text{PRE}}$ , the 4-s time bin, and the instrument background ( $F_{\text{bkg}} \sim 1$  cts/s), the significance of the excess of the each time bin should be

$$\sigma = \frac{F_{\text{accretion}}}{(F_{\text{bkg}} + F_{\text{accretion}})^{\frac{1}{2}}} \times (4N_{\text{PRE}})^{\frac{1}{2}} = 4.5. \quad (1)$$

However, we find no evidence for a hard X-ray in-

crease during the bursts, neither for IGR J17473-2721 (Chen et al. 2012), nor for 4U 1636-536 (Ji et al. 2013), nor for Aql X-1 (this paper). In contrast, we find a shortage for the non-PRE bursts, which is opposite to the expectation that the accretion rate should increase during bursts.

An enhanced persistent/accretion flux is also detected in a joint observation by Chandra and RXTE/PCA in 0.5-30 keV (Zand et al. 2013), but with more soft excess and less hard X-ray emission. They suggest that the excess in the spectra during the bursts is due to that the bursts emission being reprocessed/reflected by the disk and re-emitted into the line of sight (Ballantyne 2004). There is no conflict between the model above and our finding; i.e., during bursts, from the both observations (Worpel et al. 2013; Zand et al. 2013) in soft X-ray band and our findings in hard X-ray band, there is an increased soft X-ray flux and decreased hard X-ray flux.

This work is supported by 973 program 2009CB824800 and the National Natural Science Foundation of China via NSFC-11233003, 11103020, 11133002, 11073021 and 11173023. This work is also done in the framework of the grants AYA2012-39303, SGR2009-811, and iLINK2011-0303. DFT was additionally supported by a Friedrich Wilhelm Bessel Award of the Alexander von Humboldt Foundation. This research has made use of data obtained from the High Energy Astrophysics Science Archive Research Center (HEASARC), provided by NASA's Goddard Space Flight Center.

#### REFERENCES

- Ballantyne, D. R. 2004, *MNRAS*, 351, 57  
 Chen, Y.-P., Zhang, S., Torres, D. F., et al. 2010, *A&A*, 510, A81  
 Chen, Y.-P., Zhang, S., Torres, D. F., et al. 2011, *A&A*, 534, A101  
 Chen, Y.-P., Zhang, S., Zhang, S.-N., et al. 2012, *ApJ*, 752, L34  
 Cumming, A. 2004, *Nucl. Phys. B Proc. Suppl.*, 132, 435  
 Esin, A. A., McClintock, J. E., & Narayan, R. 1997, *ApJ*, 489, 865  
 Frank, J., King, A. & Raine, J. 2002, *Accretion Power in Astrophysics*, Cambridge Univ. Press  
 Galloway, D. K., Munro, M. P., Hartman, J. M., et al. 2008, *ApJS*, 179, 360  
 Gladstone, J., Done, C., & Gierlinski, M. 2007, *MNRAS*, 378, 13  
 Harrison, Fiona A., Boggs, Steve, Christensen, Finn et al. 2010, *Space Telescopes and Instrumentation 2010: Ultraviolet to Gamma Ray*. Edited by Arnaud, Monique; Murray, Stephen S.; Takahashi, Tadayuki. Proceedings of the SPIE, Volume 7732, pp. 77320S-77320S-8 (2010), arXiv:1008.1362  
 Ji, L., Zhang, S., Chen, Y.-P. et al. 2013, *MNRAS*, 432, 2773  
 Lewin, W. H. G., van Paradijs, J., & Taam, R. E. 1993, *Space Sci. Rev.*, 62, 223  
 Liu, B. F., Taam, Ronald E., Meyer-Hofmeister, E. 2007, *ApJ*, 671, 695  
 Maccarone, T. J. & Coppi, P. S. 2003, *A&A*, 399, 1151  
 Maitra, D., & Bailyn, C. D. 2004, *ApJ*, 608, 444  
 Mayer, M. & Pringle, J. E. 2007, *AIP Conf. Proc.* 924:760-763 (astro-ph/0612752v1)  
 Meyer, F. & Meyer-Hofmeister, E. 1994, *A&A*, 288, 175  
 Meyer-Hofmeister, E., Liu, B. F., Meyer, F., 2012, *A&A*, 544A, 87M  
 Reig, P., Méndez, M., van der Klis, M., & Ford, E. C. 2000, *ApJ*, 530, 916  
 Strohmayer, T., & Bildsten, L. 2006, *New views of thermonuclear bursts (Compact stellar X-ray sources)*, 113, 156  
 Walker, M. A. 1992, *ApJ*, 385, 642  
 Walker, M. A. & Meszaros, P. 1989, *ApJ*, 346, 844  
 Worpel, H., Galloway, D. K., Price, D. J. 2013, arXiv:1303.4824  
 Zand, J. J. M. in't, Galloway, D. K., Marshall, H. L. et al. 2013, arXiv:1301.2232Z  
 Zhang, S.-N. 2007, *Highlights of Astronomy*, 14, 41  
 Zhang, S.-N., Harmon, B. A., & Paciesas, W. S. 1996, *A&AS*, 120, 279  
 Zhang, S.-N., Cui, W., Chen, W., et al. 2000, *Science*, 287, 1239  
 Zhang, S., Chen, Y.-P., Wang, J.-M., et al. 2009, *A&A*, 502, 231

TABLE 1

AQL X-1 SELECTED BURSTS. THE COLUMNS PROVIDE INFORMATION ABOUT THE OBSID, TIME, PEAK FLUX IN 2-10 KEV (IN UNITS OF CTS/S), ON WHETHER THE BURST IS A PRE ONE OR NOT AND THE STATE WHEN THE BURSTS OCCURRED.

No	ObsID	MJD	$F_{\text{peak}}$ (cts/s)	PRE	state*
1	20098-03-08-00	50508.98	6983.32	yes	S
2	20092-01-05-00	50696.52	7188.68	yes	S
3	20092-01-05-030	50699.40	5099.40	yes	S
4	20092-01-05-07	50700.02	3776.07	no	S
5	20092-01-05-05	50701.54	3548.48	no	S
6	40047-03-02-00	51332.78	7109.68	yes	S
7	40047-03-06-00	51336.59	7177.73	yes	S
8	50049-01-04-02	51818.79	2963.57	no	H
9	50049-02-11-00	51851.40	4964.13	no	S
10	50049-02-13-01	51856.16	6223.50	yes	S
11	60054-02-01-01	52085.10	3419.08	no	H
12	60054-02-01-02	52086.04	3296.49	no	H
13	60054-02-02-01	52091.58	3227.50	no	H
14	60054-02-03-03	52100.80	5658.48	yes	S
15	60429-01-06-00	52324.99	6839.94	yes	S
16	70069-03-02-03	52347.18	5229.77	yes	S
17	70069-03-03-07	52351.88	2701.49	no	S
18	80403-01-05-00	53056.12	3158.50	no	H
19	91028-01-07-00	53468.29	3043.71	no	H
20	91028-01-09-00	53469.13	2897.51	no	H
21	91028-01-12-00	53470.99	3530.08	no	H
22	91028-01-13-00	53471.76	2795.50	no	H
23	91028-01-14-00	53472.21	2781.69	no	H
24	91028-01-18-00	53474.51	2525.70	no	H
25	91028-01-20-00	53476.03	2624.96	no	H
26	91028-01-21-00	53477.00	2761.38	no	H
27	91028-01-21-00	53477.01	992.11	no	H
28	91414-01-08-00	53715.16	3141.22	no	H
29	91414-01-08-03	53719.43	3312.39	no	H
30	91414-01-09-00	53720.16	3387.41	no	H
31	93076-01-03-00	54245.56	2395.18	no	H
32	93076-01-09-00	54251.53	3979.26	no	H
33	92438-01-02-01	54259.25	8079.84	yes	T
34	93405-01-03-07	54365.81	8005.16	yes	S
35	94076-01-04-01	55149.08	2966.77	no	H
36	94076-01-04-03	55151.19	3321.13	no	H
37	94076-01-05-02	55157.14	6655.43	yes	S
38	96440-01-09-07	55904.23	5830.69	yes	S
39	96440-01-09-01	55905.33	3577.68	no	T

State\* when the bursts occurred, S=soft state, H=hard state, T= transition state.

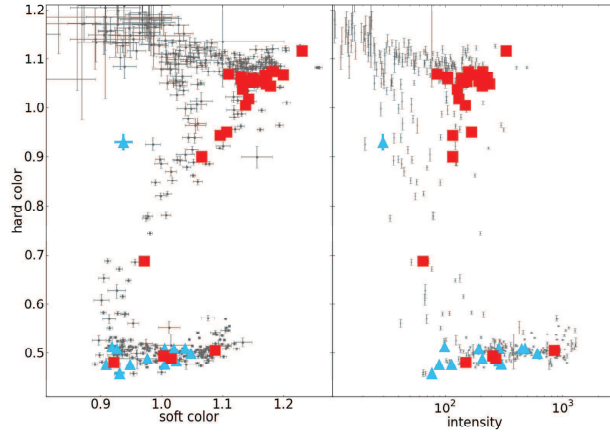


FIG. 1.— Color-color diagram (the left panel) and Hardness-Intensity diagram (the right panel) for Aql X-1. The soft color is the ratio of the background-subtracted PCA counts in the energy range 3.6-5.0 keV to the counts in the range 2.2-3.6 keV. The hard color is the ratio of counts in the ranges 8.6-18.0 and 5.0-8.6. The intensity is counts in the range 3.6-21.5 keV. The red and blue points represent the position of non-PRE bursts and PRE bursts, respectively. Each point in the diagram corresponds to an average of single OBSID for PCA, which is approximate 3000 seconds.

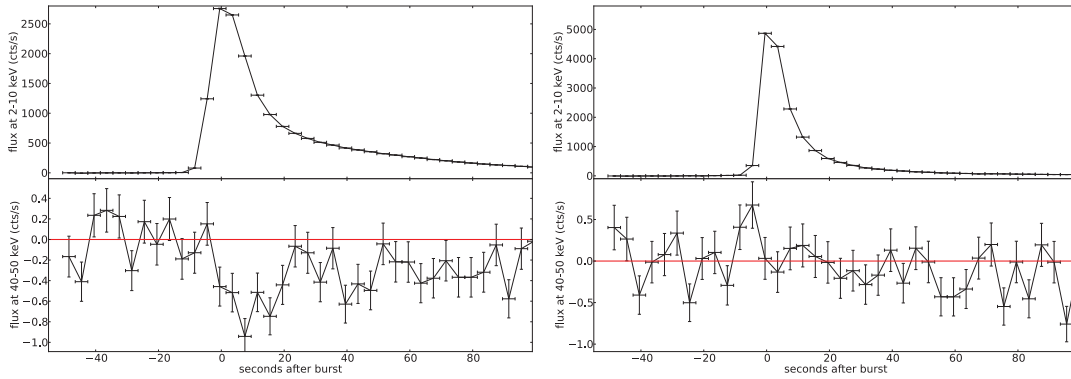


FIG. 2.— The 4s-binned lightcurves for the non-PRE bursts in the hard state (left two panels) and the PRE bursts in the soft state (right two panels). Each data point is the sum over the net lightcurve after subtracting off the persistent emissions at 2-10 keV (top panels) and 40-50 keV (bottom panels), respectively.

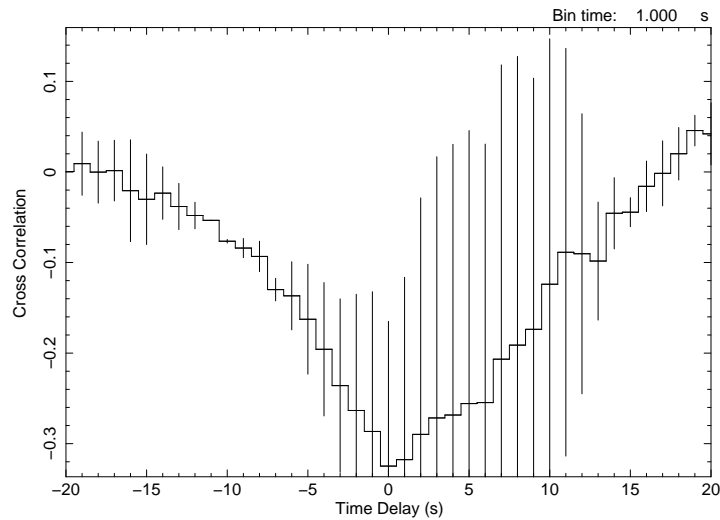


FIG. 3.— The cross-correlation between the 2-10 keV and 30-50 keV, with a time resolution of 1 second, for the combined non-PRE burst in the hard state.